Journal of Marine Systems 150 (2015) 56–65

Contents lists available at ScienceDirect

Journal of Marine Systems

journal homepage: www.elsevier.com/locate/jmarsys

Temporal changes in total and size-fractioned chlorophyll-a in surface waters of three provinces in the Atlantic Ocean (September to November) between 2003 and 2010

Ertugrul Agirbas [a,b], Victor Martinez-Vicente [b], Robert J.W. Brewin [b,c], Marie-Fanny Racault [b], Ruth L. Airs [b], Carole A. Llewellyn [b,d,*]

[a] Recep Tayyip Erdogan University, Faculty of Fisheries, 53100 Rize, Turkey
[b] Plymouth Marine Laboratory (PML), Prospect Place, The Hoe, PL1 3DH Plymouth, UK
[c] National Centre for Earth Observation, PML, Prospect Place, The Hoe, PL1 3DH Plymouth, UK
[d] Swansea University, Department of Biosciences, Singleton Park, SA2 8PP Swansea, Wales, UK

ARTICLE INFO

Article history:
Received 16 February 2015
Received in revised form 22 April 2015
Accepted 20 May 2015
Available online 27 May 2015

Keywords:
Atlantic Meridional Transect
Temporal changes
In-situ
Remote-sensing
Chlorophyll
Phytoplankton size class

ABSTRACT

Phytoplankton total chlorophyll concentration (TCHL*a*) and phytoplankton size structure are two important ecological indicators in biological oceanography. Using high performance liquid chromatography (HPLC) pigment data, collected from surface waters along the Atlantic Meridional Transect (AMT), we examine temporal changes in TCHL*a* and phytoplankton size class (PSC: micro-, nano- and pico-phytoplankton) between 2003 and 2010 (September to November cruises only), in three ecological provinces of the Atlantic Ocean. The HPLC data indicate no significant change in TCHL*a* in northern and equatorial provinces, and an increase in the southern province. These changes were not significantly different to changes in TCHL*a* derived using satellite ocean-colour data over the same study period. Despite no change in AMT TCHL*a* in northern and equatorial provinces, significant differences in PSC were observed, related to changes in key diagnostic pigments (fucoxanthin, peridinin, 19′-hexanoyloxyfucoxanthin and zeaxanthin), with an increase in small cells (nano- and pico-phytoplankton) and a decrease in larger cells (micro-phytoplankton). When fitting a three-component model of phytoplankton size structure — designed to quantify the relationship between PSC and TCHL*a* to each AMT cruise, model parameters varied over the study period. Changes in the relationship between PSC and TCHL*a* have wide implications in ecology and marine biogeochemistry, and provide key information for the development and use of empirical ocean-colour algorithms. Results illustrate the importance of maintaining a time-series of *in-situ* observations in remote regions of the ocean, such as that acquired in the AMT programme.
© 2015 Elsevier B.V. All rights reserved.

1. Introduction

Phytoplankton are responsible for ~50% of global net primary production (Field et al., 1998; Longhurst et al., 1995). Together with physical processes, phytoplankton modulate the total CO_2 concentration and pH of the ocean, and the air-sea exchange of CO_2 (Takahashi et al., 2002). Forming the base of the food web, variations in phytoplankton biomass influence the availability and transfer of energy to higher trophic levels, as illustrated by its control on global fisheries catch (Chassot et al., 2010). In addition to phytoplankton biomass, community size structure also plays a pivotal role in marine biogeochemistry. Phytoplankton cell size influences metabolic rates, growth and affinity for nutrients (Chisholm, 1992; Marañón, 2009), the structure and trophic interactions of the marine food web (Maloney and Field, 1991) and the export of carbon to the deep-ocean (Guidi et al., 2009; Laws et al., 2000). It is for these reasons that phytoplankton biomass and size structure are recognised as key ecological indicators in the marine environment (Platt and Sathyendranath, 2008). Changes in these indicators may help to detect how the marine ecosystem may respond to natural variability (*e.g.* innate climate oscillations) and human-induced change (*e.g.* anthropogenic climate change).

Total chlorophyll concentration (TCHL*a*), the major photosynthetic pigment in marine phytoplankton, is typically used as a simple metric for phytoplankton biomass, partly due to difficulties in measuring carbon biomass. TCHL*a* can be routinely estimated *in-situ* (*e.g.* fluorometrically or using High Performance Liquid Chromatography (HPLC)) or by using satellite remote-sensing of ocean colour (O'Reilly et al., 1998). Size-fractionated chlorophyll is commonly used as a metric for phytoplankton size structure and can be estimated

* Corresponding author at: Swansea University, Department of Biosciences, Singleton Park, SA2 8PP Swansea, Wales, UK. Tel.: +44 1792 606168.
E-mail address: c.a.llewellyn@swansea.ac.uk (C.A. Llewellyn).

http://dx.doi.org/10.1016/j.jmarsys.2015.05.008
0924-7963/© 2015 Elsevier B.V. All rights reserved.

through either HPLC diagnostic pigment analysis (*e.g.* Brewin et al., 2010; Devred et al., 2011; Hirata et al., 2011; Uitz et al., 2006; Vidussi et al., 2001), or through size-fractionated filtration (*e.g.* Brewin et al., 2014a, b; Marañón et al., 2012). These two techniques may be used to partition TCHL*a* into three phytoplankton size classes (PSC), micro- (>20 μm), nano- (2–20 μm) and pico-phytoplankton (<2 μm). Recent studies illustrate a tight coupling between TCHL*a*, PSC and physical forcing (Behrenfeld et al., 2006; Martinez et al., 2009; Kostadinov et al., 2010; Brewin et al., 2012). However, long-term changes in these two ecological indicators remain non-trivial to evaluate (*e.g.* Antoine et al., 2005; Boyce et al., 2010; Brewin et al., 2012; Gregg and Conkright, 2002; Kostadinov et al., 2010; Mackas, 2011; McQuatters-Gollop et al., 2011; Racault et al., 2014a; Vantrepotte & Mélin, 2009; Vantrepotte & Mélin, 2011).

Global analysis of *in-situ* data illustrates coherent relationships between PSC and TCHL*a*, which have been quantified using various statistical methods and applied to remotely-sensed observations of TCHL*a* to map PSCs at regional to global scales (Brewin et al., 2010; Brotas et al., 2013; Hirata et al., 2011; IOCCG, 2014; Marañón et al., 2012; Uitz et al., 2006; Vidussi et al., 2001). Even standard empirical algorithms used for estimating TCHL*a* from satellite ocean-colour data implicitly assume a fixed relationship between TCHL*a* and PSC (Dierssen, 2010, IOCCG, 2014). This assumption implies that a change in one indicator will result in predictable modification in the other. However, proposed statistical relationships between TCHL*a* and PSC are based on past observations and these relationships may change in a future marine ecosystem. Since these two indicators have differing roles in ecology and marine biogeochemistry, changes in the relationship between the two may have wide ramifications. Monitoring both indicators is thus required to ensure comprehensive ecosystem management (Racault et al., 2014b).

The Atlantic Meridional Transect (AMT) Programme is a UK National Environmental Research Council (NERC) funded project consisting of a time-series of oceanographic stations along a 13,500 km north–south transect (50°N–50°S) in the Atlantic Ocean (Aiken et al., 2000; Robinson et al., 2006). The AMT programme began in 1995, with the aims of quantifying the nature and causes of biogeochemical and ecological variability in plankton of the Atlantic Ocean, and assessing the effects of this variability on air–sea gas and aerosol exchange, and biological carbon cycling (Robinson et al., 2006). It was also used for the calibration and validation of measurements and products from the Sea-viewing Wide Field-of-view Sensor (SeaWiFS) (Hooker and McClain, 2000). It is one of only a few programmes that conduct systematic surveys over large areas of the ocean, crossing a range of ecosystems from the eutrophic sub-polar shelf seas and upwelling systems to the oligotrophic gyres of the North and South Atlantic. The AMT dataset includes arguably the most coherent set of repeated observations on phytoplankton pigments ever made at ocean basin scales (Aiken et al., 2009; Barlow et al., 2002; Gibb et al., 2000; Poulton et al., 2006). The objectives of this study were to: i) elucidate any change in TCHL*a* and PSC in three key ecological provinces of the Atlantic Ocean over the period 2003–2010 (September to November); and ii) investigate any change in the relationship between the two indicators (TCHL*a* and PSC) over the same period. To do this, we computed trends in TCHL*a* and PSC using surface pigment measurements collected along the AMT transect in each province. Changes in TCHL*a* were also compared with corresponding estimates from satellite ocean-colour data. The three-component model of Brewin et al. (2010), designed to quantify the relationship between TCHL*a* and PSC, was fitted to surface *in-situ* data collected along each of the AMT transects to test if the relationship between the two indicators changed over the study period. Finally, we discuss the use of empirical algorithms for the detection of TCHL*a* from satellite remote sensing and the wider implications of our results in the context of marine biogeochemistry and ecology.

2. Material and methods

2.1. HPLC pigment data

Phytoplankton pigment data from AMT cruises 13–20, covering the time period of 2003–2010, were extracted from the AMT database (https://www.bodc.ac.uk). Only pigment data between 2003 and 2010 were used (as opposed to including data from the 1995–2000 period) because: 1) the focus of our study was on changes in TCHL*a* and PSC over the past decade; 2) we wanted to limit the influence of large-scale global climate oscillations on our results, and the years 1997 and 1998 were marked by some of the largest El Niño, followed by La Niña events recorded in the past century (Wolter and Timlin, 1998), showing large impacts on global phytoplankton productivity between 1997 and 2000 (Behrenfeld et al., 2006); 3) a relatively consistent number (see Table 1) of samples were collected on AMT cruises 13–20 in the boreal Autumn; and 4) we wanted coincidental availability of *in-situ* and remote-sensing data (available post 1997). The following quality control methods were applied to the dataset:

1) For consistency with the remote-sensing data, we only retained pigment samples from the first optical depth. This depth can be approximated as $Z_{eu}/4.6$ (Gordon and McCluney, 1975), with Z_{eu} being the euphotic depth (*i.e.* the depth where Photosynthetically Available Radiation (PAR) is reduced to 1% of its value just below the surface). The euphotic depth was estimated from surface TCHL*a* using the method of Morel et al. (2007) and cross-checked with *in-situ* measurements of PAR.
2) To minimise the effect of seasonality, we separated the data collected during boreal spring and autumn (AMT cruises April–May–June and September–October–November). In our analyses, we consider pigment data from the boreal autumn only, which was collected over the 2003–2010 period (boreal spring cruises ceased from 2005). Note that September to November (boreal autumn) constitutes autumn in the northern hemisphere but spring in the southern (austral) hemisphere, and therefore, the influence of seasonality is only minimised for data within a province and not between provinces.
3) To minimise differences in cruise track sampling, we focused our analysis on open-ocean provinces that have been monitored consistently over the AMT programme. Specifically, we selected the pigment data sampled within the Longhurst (2007) biogeochemical provinces of the lower latitudes of the Atlantic Ocean: NATL (North Atlantic Gyre), TRA (Tropical Atlantic) and SATL (South Atlantic Gyre), as shown in Fig. 1.
4) Finally, we applied the method of Aiken et al. (2009) to systematically control the quality of the pigment data.

The selected 240 samples that passed these quality control procedures are listed in Table 1 for each cruise. Data in the first optical depth is also plotted for each cruise track in Fig. 1.

2.2. Pigment analysis

Water samples (1–4 l) were collected from selected depths using the rosette samples on the CTD, filtered through GF/F filters (nominal pore size 0.7 μm), flash frozen in liquid nitrogen (−196 °C), and then stored at −80 °C until the analysis was performed. Pigment analysis methods were consistent for the selected cruises (Aiken et al., 2009; Poulton et al., 2006). Phytoplankton pigments for recent AMT cruises (18–20; Airs & Martinez-Vicente, 2014a,b,c) were determined by HPLC analysis, using methods reported by Barlow et al. (1997, 2004), Tilstone et al. (2010) and Llewellyn et al. (2012), using solvent extraction and Thermo-Fisher instrumentation with photo-diode array spectroscopy (PDA) and Chromo-Quest software. Pigments were identified using retention time and spectral match PDA, and pigment concentrations were calculated using response factors generated from calibrations using a

Table 1
Available data for each cruise used in this study and corresponding method of analysis. N = number.

AMT cruise number	N of pigment data available; N of final data selected	Method of pigment analysis	Reference
AMT 13	174; 25	Barlow et al. (1997, 2004)	Aiken et al. (2009)
AMT 15	215; 24	Barlow et al. (1997, 2004)	Aiken et al. (2009)
AMT 17	144; 25	Barlow et al. (1997, 2004)	Aiken et al. (2009)
AMT 18	198; 34	Barlow et al. (1997)	Llewellyn et al. (2012)
AMT 19	110; 61	Barlow et al. (1997)	Llewellyn et al. (2012)
AMT 20	341; 71	Barlow et al. (1997)	Llewellyn et al. (2012)

suite of pigment standards (DHI Water and Environment, Denmark). Daily, pigment calibration was checked using chlorophyll-*a* and an internal standard (β-apo-8′-carotenal) was used to correct for the water content retained in the GF/F filters.

2.3. Remote-sensing data

Level 3, Standard Mapped Images of Chlorophyll-*a* were retrieved for the Atlantic Ocean at 9 km spatial resolution and at 8-day temporal resolution from the Sea-viewing Wide Field-of-View Sensor (SeaWiFS) for the period 2003 to 2010, available at http://oceancolor.gsfc.nasa.gov/. We used the reprocessing from 2010 based on the OC4v4 algorithm (Feldman, G. C., C. R. McClain, Ocean Color Web, SeaWiFS Reprocessing (2010)). To assess the spatial and temporal representativeness of discrete AMT sampling we averaged the coincident TCHL*a* from remotely-sensed 8-day composites and AMT measurements over each biogeochemical province of Longhurst (2007) during the period of each cruise. In the present study, ocean colour remote-sensing observations are used to provide a more complete appreciation of the seasonal and inter-annual variability of chlorophyll concentration in the provinces. In this context, the 8-day temporal resolution appeared to be the most relevant, balancing the finest temporal resolution and fewest missing data in the ocean-colour time series. Furthermore, statistical analysis on match-ups of satellite and *in-situ* chlorophyll concentration along AMT transects show similar results when using daily (r^2 = 0.82; for 241 match-ups, see Brewin et al. (2010)) or 8-day (r^2 = 0.80; average r^2 of six cruises, see Fig. 2 of Aiken et al. (2008)) composites.

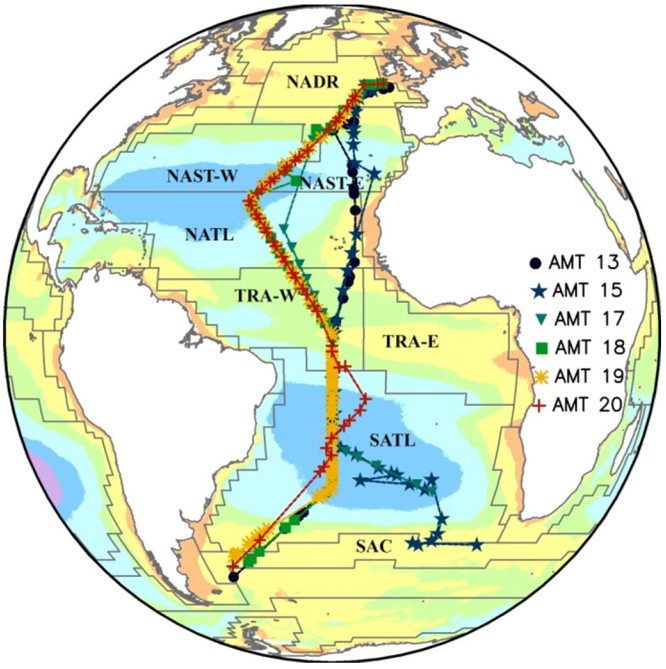

Fig. 1. AMT Cruise tracks superimposed onto the ecological provinces defined by Longhurst (2007), and the classification of Hardman-Mountford et al. (2008). NADR refers to the North Atlantic Drift province; NAST-W, -E North Atlantic Subtropical Gyre province (West, East); NATL refers to North Atlantic Tropical Gyre province; TRA-W, -E refers to Tropical Atlantic province (West, East); SATL refers to South Atlantic Gyre province; and SAC the South Atlantic Convergence province. The colours on the map refer to the biomes of Hardman-Mountford et al. (2008), with blue through to red colours referring to low to high TCHL*a*. (For interpretation of the references to color in this figure legend, the reader is referred to the web version of this article.)

2.4. Models

In addition to comparing TCHL*a* trends, we also compared trends in the fractional contribution of three phytoplankton size classes (PSC, micro-, nano- and picophytoplankton) to TCHL*a* using two models. The model of Uitz et al. (2006) was adopted, which uses *in-situ* pigment data to compute the fractions of each size class, and the model of Brewin et al. (2010), that uses *in-situ* pigment data to fit a conceptual model which is then used to re-compute the fractions of each size class from TCHL*a*.

The model of Uitz et al. (2006) involves first computing the weighted sum (ΣDPw) of the seven diagnostic pigments, such that ΣDPw = 1.41 ∗ [fucoxanthin] + 1.41 ∗ [peridinin] + 1.27 ∗ [19′ hexanoyloxyfucoxanthin] + 0.35 ∗ [19′butanoyloxyfucoxanthin] + 0.60 ∗ [alloxanthin] + 1.01 ∗ [total chlorophyll-b] + 0.86 ∗ [zeaxanthin]. The three phytoplankton size fractions were then computed according to: microphytoplankton = (1.41 ∗ [fucoxanthin] + 1.41 ∗ ∗[peridinin]) / ΣDPw; nanophytoplankton = (1.27 ∗ [19′ hexanoyloxyfucoxanthin] + 0.35 ∗ [19′butanoyloxyfucoxanthin] + 0.60 ∗ [alloxanthin]) / ΣDPw; and picophytoplankton = (1.01 ∗ [total chlorophyll-*b*] + 0.86 ∗ [zeaxanthin]) / ΣDPw.

The model of Brewin et al. (2010) was used in the following manner: (i) using the approach of Uitz et al. (2006) described above, but with the addition of a picoeukaryote adjustment (attributing part of the 19′ hexanoyloxyfucoxanthin pigment to the picophytoplankton pool at low TCHL*a*, see Brewin et al., 2010), the fractions of each size class to TCHL*a* were initially estimated; (ii) these fractions and TCHL*a* were then used to derive model parameters using a least-square-fit; and (iii) model parameters and TCHL*a* were then used to re-compute the fractions of each size class. The model of Brewin et al. (2010) was fitted to all available data in the 1st optical depth for each AMT cruise (see Fig. 2), resulting in a different set of parameters for each year and thus accounting for any potential inter-annual variation in the relationship between PSC and TCHL*a*.

2.5. Statistics

Multi-annual trends were evaluated, for each province, using linear regression analysis on $\log_{10}$-transformed TCHL*a* (Siegel et al., 2013), but not $\log_{10}$-transformed phytoplankton size fractions. The rate of TCHL*a* change over the years was calculated by transforming log-scale to linear scale. Analysis of variance (ANOVA) was used to test for significance in the trends for each province (Sokal and Rohlf, 1969). We also used a General Linear Model (GLM) to test if the intercepts and slopes of the TCHL*a* trends for *in-situ* and SeaWiFS data were significantly different.

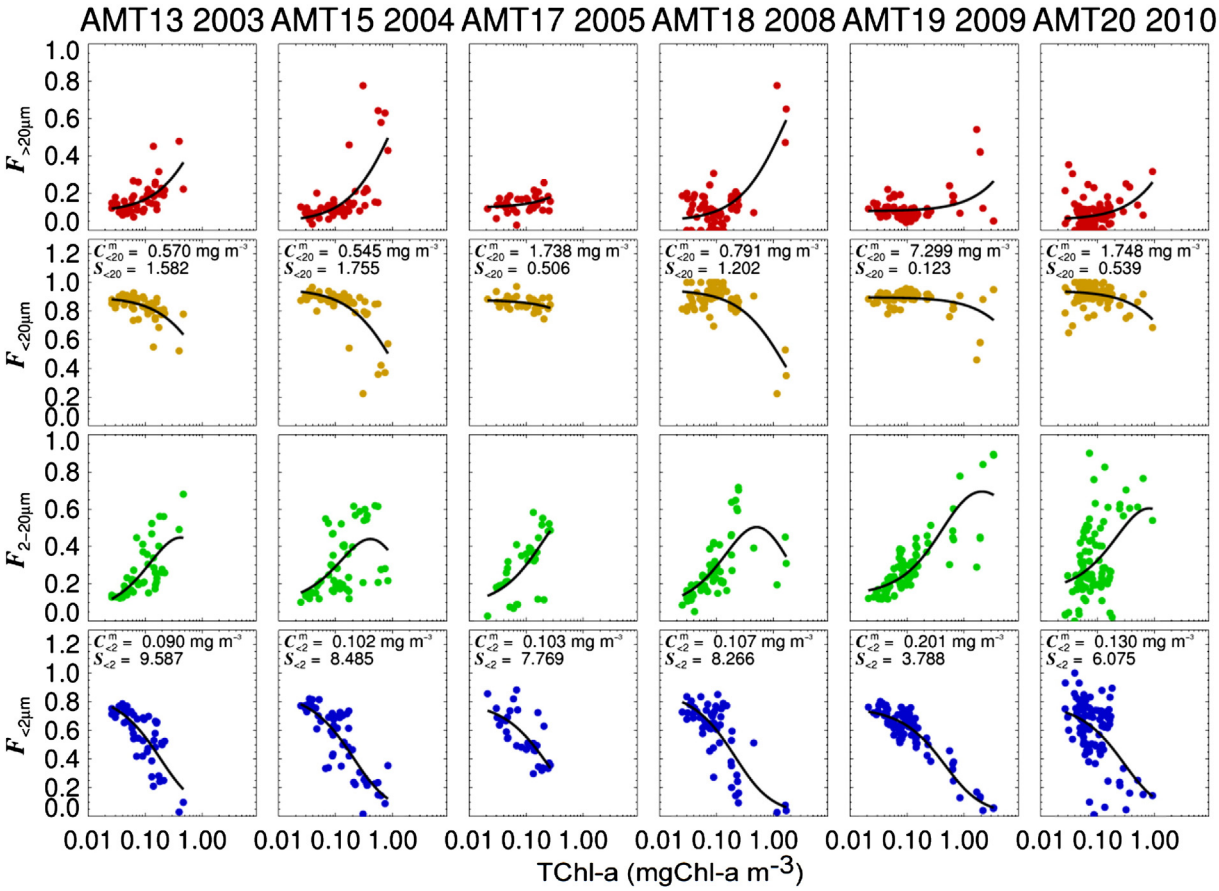

Fig. 2. The three-component model of Brewin et al. (2010), represented by the black solid line, fitted to the pigment observations from each cruise. The fractions (F) of each size class (pico- (<2 μm), nano- (2–20 μm), combined pico- and nano- (<20 μm), and micro-phytoplankton (>20 μm)) are plotted as a function of TCHL*a*. The four parameters of the model are also provided (C^m represents the maximum chlorophyll concentration for the <20 μm and <2 μm size class, and S refers to the initial slope of these two size classes, see Brewin et al. (2010) for further details).

3. Results

3.1. Total chlorophyll-a

The time-series of *in-situ* TCHL*a* are superimposed on the SeaWiFS monthly mean TCHL*a*, averaged for each province, over the 2003 to 2010 period (Fig. 3), to visualize differences in the temporal sampling rates of the two datasets. For the NATL and TRA provinces, the *in-situ* data generally lies within the spatial variability of the satellite data (quantified by the spatial standard deviation within a province, SD) at the same point of season. However, for the SATL province, the *in-situ* values are lower than SeaWiFS-derived values, probably a result of the AMT tracks passing through the most oligotrophic (centre) part of the SATL and avoiding the more productive regions at the edges of the province (Fig. 1). AMT samples were collected between September and November, which is autumn in the Northern hemisphere (NATL province) and spring in the Southern hemisphere (SATL province). Inter-annual changes in TCHL*a* may vary with season (Fig. 3), especially in provinces with changing phenology (Racault et al., 2012).

Trends in surface *in-situ* (AMT) TCHL*a* between 2003 and 2010 are plotted in Fig. 4. The *in-situ* TCHL*a* showed no significant trend in the NATL and TRA provinces, but showed a significant increase in the SATL province (0.008 ± 0.007 mg·m^{-3} year^{-1}). Trends in surface SeaWiFS-derived TCHL*a* are overlain onto the *in-situ* (AMT) trends in Fig. 4. There was a significant decline in SeaWiFS-derived TCHL*a* in the TRA (-0.009 ± 0.003 mg·m^{-3} year^{-1}) and the NATL (-0.008 ± 0.003 mg·m^{-3} year^{-1}) province during the 2003 to 2010 period. In agreement with the *in-situ* (AMT) trends, SeaWiFS-derived TCHL*a* showed a significant increase in the SATL (0.008 ± 0.003 mg·m^{-3} year^{-1}). Furthermore, General Linear Model (GLM) results revealed that inter-province differences between *in-situ* and SeaWiFS-derived TCHL*a* trends were not significant ($p > 0.05$).

3.2. Phytoplankton size fractions

The rate of change in the fractions of PSC derived using the Uitz et al. (2006) and Brewin et al. (2010) methods are plotted in Fig. 5 for the three provinces. In the NATL province both methods showed a significant decline in the microphytoplankton fractions ($p < 0.01$, Table 2), with the rate of change between -1.12% and -1.73% year^{-1}. These rates of change were not significantly different between methods (Mann–Whitney U test, Table 2). The nanophytoplankton fractions exhibited an increase of 2.47% year^{-1} ($p < 0.01$, Table 2) for the Uitz et al. (2006) method and an increase of 0.42% year^{-1} for the Brewin et al. (2010) model, with the magnitude of these increases significantly different between approaches (Mann–Whitney U test, Table 2). The rate of change in picophytoplankton fractions in the NATL was different between methods (Mann–Whitney U test, Table 2), with the Uitz et al. (2006) method showing no significant trend and the Brewin et al. (2010) model showing a significant increase (0.81% year^{-1}, $p < 0.01$, Table 2).

In the TRA province, both the Uitz et al. (2006) and Brewin et al. (2010) methods showed a significant decline in microphytoplankton fractions (-1.12% to -1.19% year^{-1}, $p < 0.01$, Table 2), no large change in the nanophytoplankton fractions, but an increase in the picophytoplankton fraction, which was significant for the Brewin et al. (2010) model (0.92% year^{-1}, $p < 0.01$, Table 2). In the SATL province,

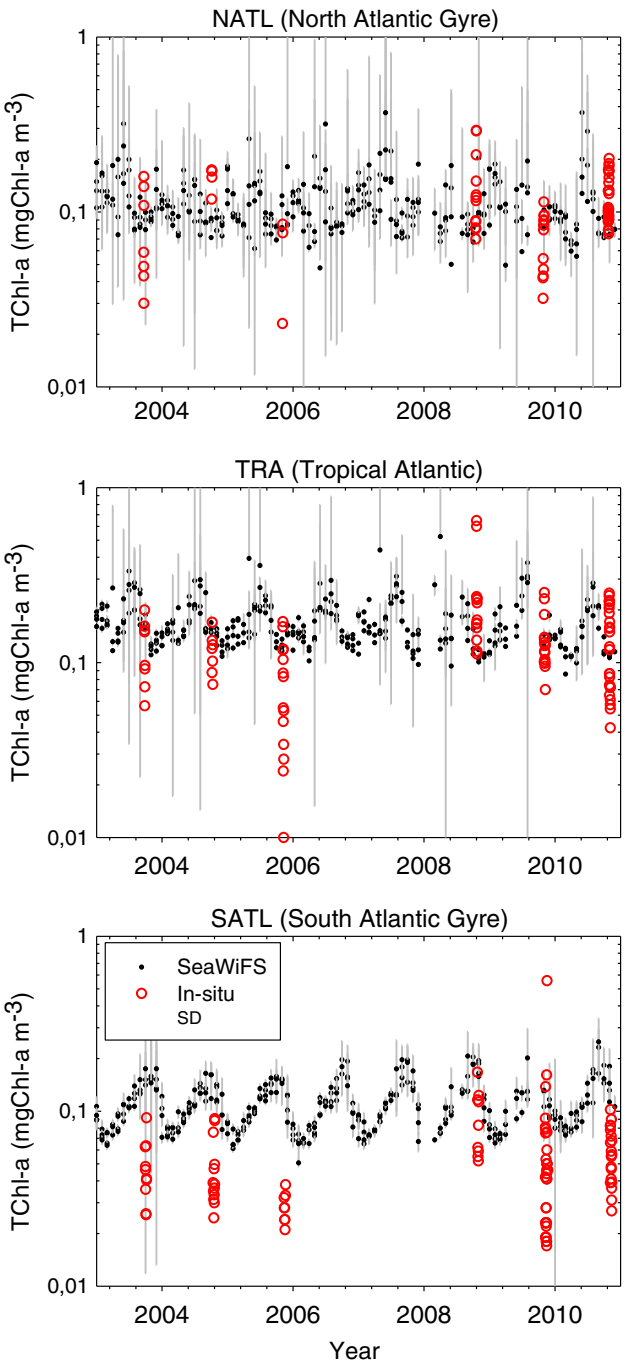

Fig. 3. Time series of TCHL*a* (*in-situ* HPLC TCHLa from AMT sampling and satellite TCHLa from SeaWiFS sensor) for each of the three provinces (grey lines represent standard deviations across the province for the SeaWiFS image, SD).

the Brewin et al. (2010) and Uitz et al. (2006) methods varied slightly, though these variations were not significantly different according to the Mann–Whitney U test (Table 2). The Brewin et al. (2010) model indicated a decreasing trend in the SATL microphytoplankton fractions, not observed in the Uitz et al. (2006) method (Fig. 5, Table 2). The Uitz et al. (2006) approach indicated a decline in SATL nanophytoplankton fractions (-1.45% year^{-1}, $p < 0.01$) that was not observed in the Brewin et al. (2010) approach. Both methods showed a significant increase in the picoplankton fraction in the SATL (Fig. 5, Table 2).

The parameters of the Brewin et al. (2010) model were found to vary among cruises (Fig. 2), implying a modification in the relationship between PSC and TCHL*a* over the time period. In fact, the parameters

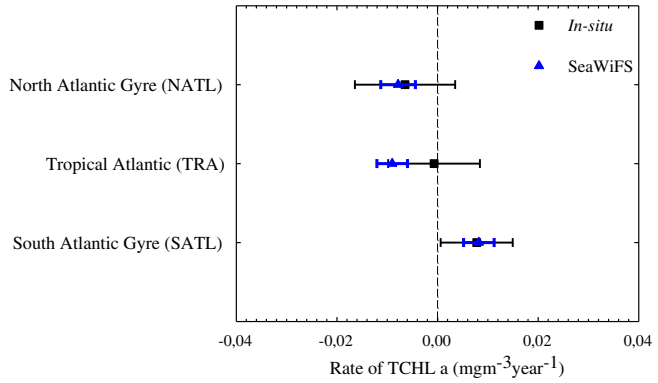

Fig. 4. Mean instantaneous rates of *in-situ* and SeaWiFS TCHL*a* change estimated for each province with 95% confidence limits.

representing the maximum chlorophyll concentration for the <20 μm and <2 μm size class (denoted $C^{m}_{<20\ \mu m}$ and $C^{m}_{<2\ \mu m}$ in Fig. 2) were positively correlated with time ($r = 0.52$ and 0.67 respectively), and

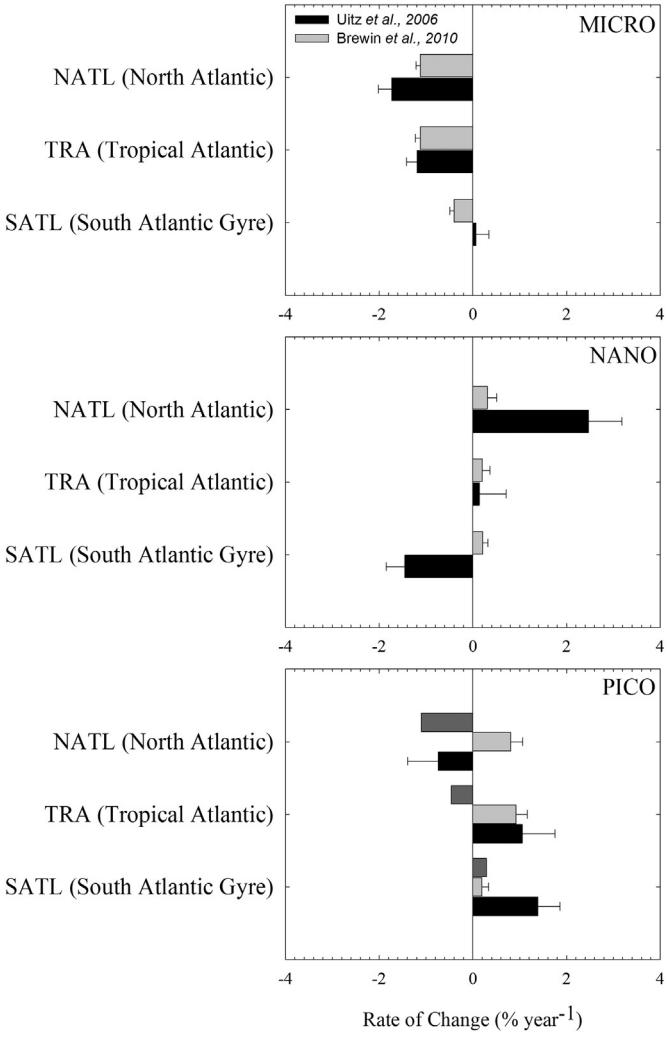

Fig. 5. Rates of change in PSC, for *in-situ* (Uitz et al. 2006) and model-derived (Brewin et al. 2010) data, together with 95% confidence limits.

Table 2
Average percentages (±standard errors) for *in-situ* and model derived Phytoplankton Size Classes (PSC) in the first optical depth for the different AMT cruises and biogeochemical provinces.

Province/cruise	Microphytoplankton			Nanophytoplankton		Picophytoplankton	
	N	Uitz et al.	Brewin et al.	Uitz et al.	Brewin et al.	Uitz et al.	Brewin et al.
NATL							
AMT-13	7	15 ± 1.2	15 ± 1.2	26 ± 2.5	30 ± 1.4	59 ± 3.2	55 ± 2.6
AMT-15	4	20 ± 8.8	16 ± 0.9	16 ± 1.7	36 ± 0.7	64 ± 7.4	47 ± 1.6
AMT-17	3	14 ± 0.8	15 ± 0.8	37 ± 0.6	36 ± 2.3	49 ± 1.3	50 ± 3.1
AMT-18	12	8.9 ± 1.7	9.8 ± 0.8	29 ± 1.0	31 ± 1.3	63 ± 2.2	60 ± 2.0
AMT-19	12	8.9 ± 0.3	11 ± 0.1	29 ± 2.1	29 ± 0.3	62 ± 2.1	60 ± 0.3
AMT-20	27	4.3 ± 0.8	7.9 ± 0.2	43 ± 3.7	35 ± 0.5	53 ± 3.2	57 ± 0.6
N (per province)	65						
ANOVA		$p < 0.01$	$p < 0.01$	$p < 0.01$	$p < 0.01$	NS	$p < 0.01$
Mann–Whitney		NS		$p < 0.01$		$p < 0.01$	
TRA							
AMT-13	8	14 ± 2.0	18 ± 1.1	22 ± 1.1	33 ± 1.1	68 ± 2.3	49 ± 2.2
AMT-15	7	12 ± 0.7	14 ± 0.9	29 ± 6.5	34 ± 0.8	59 ± 6.8	52 ± 1.6
AMT-17	14	16 ± 1.4	15 ± 0.4	28 ± 4.5	36 ± 1.1	56 ± 5.0	49 ± 1.6
AMT-18	13	4.5 ± 1.0	12 ± 1.3	22 ± 1.7	34 ± 1.2	73 ± 2.2	55 ± 2.5
AMT-19	17	8.6 ± 0.5	11 ± 0.1	31 ± 2.1	33 ± 0.6	61 ± 2.5	57 ± 0.7
AMT-20	25	7.6 ± 1.2	8.5 ± 0.2	25 ± 3.3	37 ± 0.6	67 ± 4.2	55 ± 0.9
N (per province)	84						
ANOVA		$p < 0.01$	$p < 0.01$	NS	$p < 0.01$	NS	$p < 0.01$
Mann–Whitney		$p < 0.05$		$p < 0.01$		$p < 0.01$	
SATL							
AMT-13	10	11 ± 1.1	13.24 ± 0.4	29 ± 1.9	27 ± 0.6	60 ± 2.6	60 ± 1.0
AMT-15	13	9.4 ± 1.1	8.31 ± 0.5	31 ± 1.5	29 ± 0.6	60 ± 2.1	63 ± 1.1
AMT-17	8	15 ± 1.2	13.05 ± 0.1	39 ± 4.4	31 ± 0.2	47 ± 4.2	56 ± 0.39
AMT-18	9	13 ± 3.8	8.46 ± 0.5	30 ± 3.4	28 ± 1.1	57 ± 4.8	63 ± 1.6
AMT-19	32	12 ± 0.8	10.59 ± 0.1	26 ± 0.8	27 ± 0.3	63 ± 1.1	63 ± 0.3
AMT-20	19	11 ± 2.4	7.09 ± 0.1	19 ± 3.4	33 ± 0.4	70 ± 3.9	60 ± 0.6
N (per province)	91						
ANOVA		NS	$p < 0.01$	$p < 0.01$	$p < 0.01$	$p < 0.01$	$p < 0.01$
Mann–Whitney		NS		NS		NS	

Data include first optical depth *in-situ* and model derived PSC. Biogeochemical provinces included are NATL (North Atlantic Gyre), TRA (Tropical Atlantic) and SATL (South Atlantic Gyre). N indicates number of data used in analyse. One-way ANOVA is used to analyse inter-cruise differences for all data; Mann–Whitney U test is used to analyse *in-situ* and model derived PSC differences. NS indicates not significant.

the initial slopes of the model ($S_{<20\ \mu m}$ and $S_{<2\ \mu m}$ in Fig. 2) negatively correlated with time ($r = -0.71$ and -0.78 respectively). However, given that there were only six parameters (one set for each cruises), these correlations were not statistically significant ($p > 0.05$).

3.3. Phytoplankton pigment ratios

To understand further the variability in PSC over the study period, we looked at trends in different marker pigment ratios in the three provinces (Fig. 6). The ratio of both fucoxanthin (the main indicator for diatoms, may also be found in some flagellates) and peridinin (the main indicator of dinoflagellates) to the sum of diagnostic pigments (DP) significantly declined in the NATL and TRA provinces (Fig. 6, Table 3), reflecting changes in PSC in both the Brewin et al. (2010) and Uitz et al. (2006) methods (Fig. 5).

Changes in the nanophytoplankton fractions (Fig. 5) were further investigated by examining the representative pigment ratios of 19′ hexanoyloxyfucoxanthin (marker for haptophytes, Jeffrey et al., 2011), 19-butanoyloxyfucoxanthin (marker for pelagophytes, Jeffrey et al., 2011) and alloxanthin (marker for cryptophytes). The largest changes were observed in ratio of 19′hexanoyloxyfucoxanthin to DP (haptophytes), with a significant increase in the NATL and decrease in the SATL (Fig. 6, Table 3). These changes mimic the changes observed in the nanophytoplankton fraction using the Uitz et al. (2006) method in all provinces (Fig. 5), and also reflect the increase in the picophytoplankton fraction in the NATL for the Brewin et al. (2010) model, when considering that in the process of parameterising this model the 19′hexanoyloxyfucoxanthin pigment is attributed to picophytoplankton at low TCHL*a* (picoeukaryote adjustment).

Changes in the picophytoplankton fractions (Fig. 5) were further investigated by examining TCHL*b* (marker for green flagellates and prochlorophytes) and zeaxanthin (marker for cyanobacteria and prochlorophytes) pigment ratios (Fig. 6). In general, changes in zeaxanthin/DP reflect the trends in PSC using the Uitz et al. (2006) method in all three provinces, and also the Brewin et al. (2010) model in the TRA, indicating the important role of prochlorophytes and cyanobacteria in this size range. The smaller increase in picophytoplankton fractions (Fig. 5) in SATL using the Brewin et al. (2010) model (Fig. 5), when compared with the Uitz et al. (2006) method, is likely related to a conflicting increase in zeaxanthin/DP and decrease in 19′hexanoyloxyfucoxanthin/DP, both of with are attributed to picophytoplankton at low TCHL*a* when parameterising this model. This likely reflects an increase in prochlorophytes and cyanobacteria, with respect to picoeukaryotes, in this province.

4. Discussion

4.1. Trends in total chlorophyll-a

Over the 2003 to 2010 period, there was no significant trend in AMT *in-situ* TCHL*a* in the NATL and TRA provinces, but there was a significant increase in the SATL province. The eight-year time-period is too short to deduce any long-term trends in TCHL*a*, especially when considering a continuous time-series of ~40 years in length is required to distinguish a global warming trend from natural variability (Henson et al., 2010), and considering our results are only representative of the September to November period.

Although our results are not directly comparable to other estimates of trends in TCHL*a* based on datasets collected over much longer time-

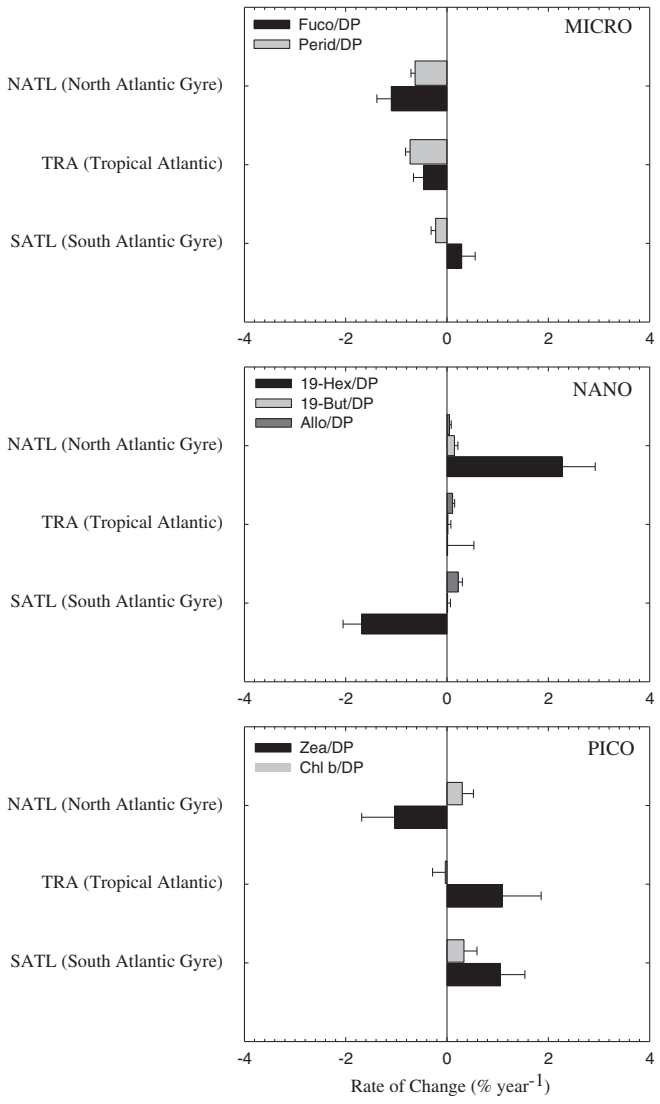

Fig. 6. Rates of change in marker pigment ratios in the three provinces, together with 95% confidence limits.

periods, it is useful to place our findings the context of current literature. Boyce et al. (2014) report significant declines in TCHL*a* in the North West Atlantic, Eastern Atlantic and South Atlantic over the past century, using a dataset of merged Secchi disc observations, Forel–Ule (FU) colour data, and TCHL*a* data (Boyce et al., 2010, 2012). Boyce et al. (2014) also report a significant increase in TCHL*a* in the North East Atlantic, in agreement with trends presented by Raitsos et al. (2005, 2014) and McQuatters-Gollop et al. (2011), derived using the Continuous Plankton Recorder (CPR) Phytoplankton Colour Index (PCI). However, conflicting results from these studies were presented in the central Northeast Atlantic. All these studies involve the use of proxies for TCHL*a*, which have limitations. PCI, Secchi disc and FU observations are visual estimates and limited by differences in the psychophysiology of the human eye–brain system. Both Secchi disc and FU data are vulnerable to variations in the relationships between TCHL*a* and other optically-significant water constituents (*e.g.* coloured-dissolved material and non-algal particles). The CPR has a mesh size of ~270 μm, and therefore may fail to capture the smaller phytoplankton biomass (*e.g.* pico- and nano-phytoplankton). Also, the Boyce et al. (2014) study involves blending different types of data, which if not carefully dealt with can lead to biases in the results (Boyce et al., 2014; Mackas, 2011). In our study, we used high quality HPLC estimates of TCHL*a* (not proxies) that were processed consistently over the entire study period, and therefore less vulnerable to the issues raised in these studies.

Trends in the three provinces observed in the *in-situ* AMT data were not significantly different to trends in SeaWiFS-derived TCHL*a*, supporting the use of AMT data as a platform for TCHL*a* trend detection, despite only sampling a limited area within each province (Fig. 1). However, SeaWiFS-derived TCHL*a* indicated significant declines in NATL and TRA, not observed in the AMT data. Furthermore, whereas recent long-term analysis (>10 years) of SeaWiFS-derived TCHL*a* indicates a decrease over the entire NATL province, regions of both increase and decrease have been observed in the TRA and SATL (Siegel et al., 2013; Vantrepotte & Mélin, 2009), suggesting variability in trends within these two provinces that may not be captured on a specific AMT transect route. Confidence in the satellite estimates of SeaWiFS TCHL*a* can be taken from the fact that they compare favourably with weekly and daily AMT match-ups (Aiken et al., 2009; Brewin et al., 2010). Furthermore, seasonal and inter-annual variations (including trends) in SeaWiFS TCHL*a* are consistent with those derived using the MODIS-Aqua and MERIS ocean-colour sensors over a similar time-period (2002–2010; see Brewin et al., 2014c), lending confidence to the SeaWiFS results. Blending *in-situ* and satellite observations of TCHL*a* (*e.g.* AMT and SeaWiFS) may lead to more robust estimates of trends (Aiken et al., 2009; Gregg & Casey, 2010; Gregg & Rousseaux, 2014) and minimise the impact of periods of missing data (Beaulieu et al., 2013; Racault et al., 2014a).

Difficulties arise when comparing our results on inter-annual variability in TCHL*a* and PSC with results from earlier AMT studies, given differences in cruise tracks and sampling periods. Gibb et al. (2000) compared pigment data collected during 1996 (AMT 2 and 3) with data collected during 1997 (AMT 4 and 5). They found an increase in the concentration of pigments associated with picoplankton (sum of zeaxanthin and divinyl chlorophyll a) during 1997 (AMT 4 and 5), particularly in the equatorial provinces, suggesting an increase in smaller size classes, consistent with our findings during the 2003–2010 period. However, changes between 1996 and 1997 were likely a result of the large El Niño event that occurred (Wolter and Timlin, 1998), which impacted global phytoplankton productivity and phytoplankton size structure (Behrenfeld et al., 2006, Kostadinov et al. 2010). Aiken et al. (2009) reported low inter-annual variability in TCHL*a* in all provinces between the 1996–2006 period, but observed evidence of an El Niño perturbation between 1997 and 1998, and a downward trend from 1998–2003, consistent with global changes reported by Behrenfeld et al. (2006). Multi-decadal datasets are required to partition the influence of shorter term variability (*e.g.* El Niño) on long term trends, which can only be acquired through the continuation of programmes such as the AMT.

4.2. Implications of modifications in the relationship between PSC and TCHLa

There are discrepancies in the use of diagnostic pigments to infer phytoplankton size structure. Some diagnostic pigments such as fucoxanthin (main indicator of diatoms) may also be found in some flagellates (Jeffrey et al., 2011; Vidussi et al., 2001) and the pigment groupings do not strictly reflect the true size of phytoplankton (Uitz et al., 2006). Brewin et al. (2014a) conducted a comparison of size-fractionated chlorophyll estimated independently from HPLC diagnostic pigment analysis and from size-fractionated filtration (SFF) along the AMT transect. Encouragingly, they found size-fractionated chlorophyll estimated from HPLC and SFF data were significantly correlated, with HPLC data explaining between 40% and 88% of the variability in the SFF data. However, there were biases between the two methods, with HPLC methods overestimating nanophytoplankton chlorophyll and underestimating picophytoplankton chlorophyll when compared with SFF. Brotas et al. (2013) compared size-fractionated chlorophyll derived using the Brewin et al. (2010) model, parameterised using HPLC

Table 3
Average diagnostic pigment ratios (in percentage with ± standard errors) for *in-situ* data in the first optical depth for the different AMT cruises and biogeochemical provinces.

Province/cruise	N	Fuco/DP	Perid/DP	Zea/DP	Chlb/DP	19-Hex/DP	19-But/DP	Allo/DP
NATL								
AMT-13	7	10 ± 1.2	5.0 ± 0.4	58 ± 3.3	1.5 ± 0.8	23 ± 2.1	2.6 ± 0.4	0.1 ± 0.1
AMT-15	4	16 ± 9.0	3.2 ± 0.4	64 ± 7.4	–	15 ± 1.6	1.1 ± 0.1	0.1 ± 0.1
AMT-17	3	8.0 ± 0.6	6.0 ± 0.2	46 ± 0.4	3.3 ± 1.7	34 ± 0.6	2.2 ± 0.2	0.5 ± 0.3
AMT-18	12	7.5 ± 1.6	1.4 ± 0.8	57 ± 1.9	5.8 ± 1.8	26 ± 0.9	2.3 ± 0.2	0.1 ± 0.1
AMT-19	12	5.7 ± 0.3	3.2 ± 0.2	55 ± 2.4	7.4 ± 0.3	27 ± 2.0	1.8 ± 0.1	1.9 ± 0.1
AMT-20	27	4.2 ± 0.8	0.1 ± 0.1	50 ± 3.2	2.4 ± 0.8	39 ± 3.4	3.3 ± 0.3	0.4 ± 0.2
ANOVA		$p < 0.01$	$p < 0.01$	NS	$p < 0.01$	$p < 0.01$	$p < 0.01$	NS
TRA								
AMT-13	8	8.4 ± 1.5	6.0 ± 1.1	58 ± 2.8	5.3 ± 0.8	20 ± 1.0	1.6 ± 0.1	0.1 ± 0.1
AMT-15	7	6.8 ± 0.9	5.3 ± 0.9	59 ± 6.8	–	26 ± 5.5	2.8 ± 0.9	–
AMT-17	14	12 ± 1.2	4.7 ± 0.8	52 ± 5.3	4.2 ± 1.3	25 ± 4.1	1.7 ± 0.5	0.8 ± 0.2
AMT-18	13	4.1 ± 0.9	0.4 ± 0.4	68 ± 4.7	5.6 ± 2.8	21 ± 1.3	1.5 ± 0.5	0.1 ± 0.1
AMT-19	17	5.8 ± 0.4	2.8 ± 0.9	51 ± 2.4	9.5 ± 0.8	28 ± 2.0	2.0 ± 0.2	0.5 ± 0.1
AMT-20	25	7.0 ± 1.2	0.6 ± 0.2	67 ± 4.2	0.6 ± 0.3	22 ± 3.0	2.1 ± 0.2	1.2 ± 0.3
ANOVA		$p < 0.01$	$p < 0.01$	$p < 0.05$	$p < 0.01$	NS	NS	$p < 0.01$
SATL								
AMT-13	10	7.1 ± 0.6	4.1 ± 0.7	53 ± 3.3	7.3 ± 3.2	26 ± 1.8	2.7 ± 0.2	0.1 ± 0.1
AMT-15	13	7.8 ± 0.9	1.7 ± 0.4	59 ± 2.3	0.6 ± 0.4	28 ± 1.4	3.1 ± 0.2	–
AMT-17	8	9.5 ± 1.3	5.0 ± 1.3	41 ± 4.0	5.9 ± 2.0	35 ± 4.5	3.1 ± 0.5	0.5 ± 0.5
AMT-18	9	12 ± 3.9	1.0 ± 0.7	51 ± 5.0	5.9 ± 1.5	27 ± 3.2	3.5 ± 0.4	0.1 ± 0.1
AMT-19	32	8.1 ± 0.8	3.5 ± 0.2	56 ± 0.9	6.7 ± 0.5	22 ± 0.7	2.3 ± 0.1	1.3 ± 0.1
AMT-20	19	11 ± 2.3	0.6 ± 0.3	64 ± 3.8	5.7 ± 2.2	14 ± 3.0	3.6 ± 0.6	1.7 ± 1.0
ANOVA		NS	$p < 0.01$	$p < 0.01$	NS	$p < 0.01$	$p < 0.05$	NS

Data include first optical depth pigment ratios for different size fractions (Fuco: fucoxanthin, Perid: peridinin, Zea: zeaxanthin, Chlb: chlorophyll b, 19-Hex: 19-hexanoyloxyfucoxanthin, 19-But: 19-butanoyloxyfucoxanthin, Allo: alloxanthin, DP: diagnostic pigments (Fuco + Perid + Zea + Chlb + 19-Hex + 19-But + Allo)). Biogeochemical provinces included are NATL (North Atlantic Gyre), TRA (Tropical Atlantic) and SATL (South Atlantic Gyre). N indicates number of data used in analyse. One-way ANOVA is used to analyse inter-cruise differences for all data. NS indicates not significant.

diagnostic pigment analysis, with cell counts estimated from flow cytometry and microscopy. Their estimated cellular TCHL*a* values for the three size classes (pico-, nano- and microphytoplankton) were consistent with literature values derived from laboratory cultures, providing an indirect validation of the diagnostic pigment method to assign size classes. These studies provide some confidence in the use diagnostic pigments to infer PSC. However, additional analysis is required to quantify uncertainties in this pigment-based approach (Brewin et al., 2014a).

Significant temporal changes in PSC were observed in the NATL and TRA provinces (Fig. 5), despite no significant change in TCHL*a* (Fig. 4). In both provinces, there was evidence of a decrease in the fraction of microphytoplankton to TCHL*a*, and evidence of an increase in the fraction of nano- and picophytoplankton (Fig. 5). A significant increase in TCHL*a* in the SATL province (Fig. 4) was also at odds with an increase in the fraction picophytoplankton to TCHL*a* (Fig. 5), which are typically inversely related (*e.g.* see Fig. 2). Furthermore, when fitting the model of Brewin et al. (2010) to each AMT cruise individually (all data within the 1st optical depth), we observed changes in model parameters (Fig. 2), consistent with a change in the relationship between PSC and TCHL*a* over the study period.

When considering the different roles of these two ecological indicators, changes in the relationship between PSC and TCHL*a* may have wide implications in marine biogeochemical cycling. Picophytoplankton absorb light with higher efficiency than larger phytoplankton (Brewin et al., 2011; Ciotti et al., 2002; Devred et al., 2011; Uitz et al., 2008), therefore, for the same TCHL*a*, an increase in the picophytoplankton fraction would result in an increase in the absorption of incoming radiation which could impact light availability for photosynthesis and heating of the upper ocean. The photophysiology of phytoplankton is influenced by its size structure (Uitz et al., 2008); such that changes in the relationship between PSC and TCHL*a* are likely to influence the relationship between TCHL*a* and primary production (Uitz et al., 2010). Microphytoplankton are generally positively correlated with new and export production (Dugdale et al., 2007; Guidi et al., 2009; Uitz et al., 2010) and picophytoplankton with recycled production (Chisholm, 1992). For the same level of TCHL*a*, one may expect modifications in recycled, new and export production with changes in PSC. The amount of carbon exported or recycled in the upper ocean impacts the CO_2 concentrations and pH of the ocean, affecting air–sea CO_2 gas transfer, and potentially the role of the ocean as a sink for increasing atmospheric CO_2.

Analysis of phytoplankton pigment ratios indicates modifications in the composition of fucoxanthin, peridinin, 19′-hexanoyloxyfucoxanthin and zeaxanthin in the three provinces over the study period (Fig. 6), indicative of modifications in diatoms, dinoflagellates, haptophytes and prokaryotes respectively. There is evidence that the phytoplankton community influences the transfer of energy through the food-web and the type of fish that prosper in a given environment (Beaugrand, 2003; Beaugrand & Reid, 2003, IOCCG, 2014). For instance, in the Benguela upwelling diatoms are correlated with the growth of anchovy while flagellates are correlated with the growth of sardines (Cury et al., 2008). Strong correlations have been observed between the occurrence of diatoms and the anchovy catch in the Humboldt ecosystem (Jackson et al., 2011). The distribution and rate of synthesis of essential fatty acids, required by all vertebrates, has been found to vary with diatom occurrence (Budge et al., 2014). Careful monitoring of phytoplankton community structure is required to ensure sustainable management of fisheries (IOCCG, 2014).

Other biogeochemical cycles are also likely to be influenced by modifications in the composition of the phytoplankton community relative to TCHL*a*. For instance, diatoms influence the cycling of silicate (Kröger et al., 2000), some prymnesiophyte species (such as coccolithophores) impact the cycling of calcium carbonate (Morse et al., 2007) and some (such as *Phaeocystis antarctica*) produce dimethyl sulphide (DMS; Liss et al., 1994). Cyanobacteria, such as *Trichodesmium*, utilise N_2 from the atmosphere and thus influence the nitrogen cycle (Falkowski, 1997; Tyrrell, 1999). Comprehensive monitoring of phytoplankton community structure is required to better understand important biogeochemical processes and how they may respond to climate variability and change (IOCCG, 2014; Le Quéré et al., 2005).

Changes in the relationship between phytoplankton community structure and TCHL*a* will also influence the use of empirical ocean-

colour remote-sensing algorithms. For instance, it has been shown that information on the absorption and backscattering properties of phytoplankton size is implicit in remote-sensing algorithms that empirically relate TCHL*a* to band-ratio reflectance (Dierssen, 2010; IOCCG, 2014). In fact, these algorithms implicitly assume a fixed relationship between PSC and TCHL*a* (IOCCG, 2014). Modifications in this relationship will likely impact the accuracy of these empirical algorithms. This presents a challenge for ocean-colour remote-sensing, as a change in ocean colour can occur from either a change in community composition (*e.g.* PSC) or in TCHL*a*. Empirical relationships, that tie one indicator to the next, need to be minimised in models, since correlations between elements of the ecosystem may not be stable in a changing climate (Figs. 4 and 5). If empirical relationships are unavoidable, on-going recalibration is required to reduce ambiguity in interpretation of results, since empirical relationships based on past observations may not be a faithful guide to the future state of the ocean. Such recalibrations cannot occur without high quality *in-situ* observations, such as those acquired in the AMT programme.

This study has demonstrated that the relationship between PSC and TCHL*a* may vary between years, and given that PSC and TCHL*a* have differing roles in ecology and marine biogeochemistry, long-term monitoring of both indicators is required to ensure comprehensive ecosystem management. The AMT programme, soon to reach its 20th year, is one of a few oceanographic programmes capable of monitoring these indicators over basin-wide scales and delivering the measurements required for global ecosystem management. It is vital that such programmes are sustained long into the future.

5. Conclusions

Making use of surface pigment data collected on the Atlantic Meridional Transect (AMT) between 2003 and 2010 (September to November period only), we examine temporal changes in total chlorophyll-*a* (TCHL*a*) and phytoplankton size classes (PSC; micro-, nano- and picophytoplankton, estimated from pigment analysis) in three ecological provinces of the Atlantic Ocean. No significant changes were observed in TCHL*a* in northern (NATL) and equatorial provinces (TRA), but a significant increase was observed in the southern province (SATL). These changes were not significantly different to those derived using satellite data (SeaWiFS) over the same study period.

Despite no change in TCHL*a* in the NATL and SATL, significant changes were observed in PSC, with increases in small cells (pico- and nanophytoplankton) and decreases in large cells (microphytoplankton) in these provinces. These changes were related to modifications in key phytoplankton diagnostic pigments (principally fucoxanthin, peridinin, 19′-hexanoyloxyfucoxanthin and zeaxanthin). We also observed changes in the parameters of a three-component model over the study period which relates PSC to TCHL*a*. Results indicate a change in the relationship between PSC and TCHL*a* during this eight-year period, which has wide implications for ecosystem structure, marine biogeochemistry and ocean-colour remote sensing, and illustrates the importance of the AMT programme in monitoring the health of Atlantic Ocean ecosystem.

Acknowledgements

Data was used from the Atlantic Meridional Transect (AMT) Consortium (NER/0/5/2001/00680), provided by the British Oceanographic Data Centre (BODC) and supported by the Natural Environment Research Council National Capability funding to Plymouth Marine Laboratory and the National Oceanography Centre, Southampton. We sincerely thank officers and crew of the RRS James Clark Ross, RRS James Cook and RRS Discovery, for their help during the AMT cruises and all those involved in pigment data collection and analysis. We also thank Alex J. Poulton for comments on the manuscript. This is contribution number 272 of the AMT programme.

References

Aiken, J., Rees, N., Hooker, S., Holligan, P., Bale, A., Robins, D., Moore, G., Harris, R., Pilgrim, D., 2000. The Atlantic Meridional Transect: overview and synthesis of data. Prog. Oceanogr. 45 (3–4), 257–312.

Aiken, J., Pradhan, Y., Barlow, R., Lavender, S., Poulton, A., Holligan, P., Hardman-Mountford, N., 2009. Phytoplankton pigments and functional types in the Atlantic Ocean: a decadal assessment, 1995–2005. Deep-Sea Res. II Top. Stud. Oceanogr. 56 (15), 899–991.

Aiken, J., Hardman-Mountford, N.J., Barlow, R., Fishwick, J.R., Hirata, T., Smyth, T.J., 2008. Functional links between bioenergetics and bio-optical traits of phytoplankton taxonomic groups: An overarching hypothesis with applications for ocean colour remote sensing. J. Plankton Res. 30 (2), 165–181.

Airs, R., Martinez-Vicente, V., 2014a. AMT18 (JR20081003) HPLC Pigment Measurements From CTD Bottle Samples. British Oceanographic Data Centre — Natural Environment Research Council, UK (doi:10/tk2).

Airs, R., Martinez-Vicente, V., 2014b. AMT19 (JC039) HPLC Pigment Measurements From CTD Bottle Samples. British Oceanographic Data Centre — Natural Environment Research Council, UK (doi:10/tk3).

Airs, R., Martinez-Vicente, V., 2014c. AMT20 (JC053) HPLC Pigment Measurements From CTD Bottle Samples. British Oceanographic Data Centre — Natural Environment Research Council, UK (10/tk4).

Antoine, D., Morel, A., Gordon, H.R., Banzon, V.F., Evans, R.H., 2005. Bridging ocean color observations of the 1980s and 2000s in search of long-term trends. J. Geophys. Res. 110, C06009. http://dx.doi.org/10.1029/2004JC002620.

Barlow, R.G., Cummings, D.G., Gibb, S.W., 1997. Improved resolution of mono- and divinyl chlorophylls a and b and zeaxanthin and lutein in phytoplankton extracts using reverse phase C-8 HPLC. Mar. Ecol. Prog. Ser. 161, 303–307.

Barlow, R.G., Aiken, J., Holligan, P.M., Cummings, D.G., Maritorena, S., Hooker, S., 2002. Phytoplankton pigment and absorption characteristics along meridional transects in the Atlantic Ocean. Deep-Sea Res. I Oceanogr. Res. Pap. 49 (4), 637–660.

Barlow, R.G., Aiken, J., Moore, G.F., Holligan, P.M., Lavender, S., 2004. Pigment adaptations in surface phytoplankton along the eastern boundary of the Atlantic Ocean. Mar. Ecol. Prog. Ser. 281, 13–26.

Beaugrand, G., 2003. Plankton effect on cod recruitment in the North Sea. Nature 426, 661–664.

Beaugrand, G., Reid, P., 2003. Long-term changes in phytoplankton, zooplankton and salmon related to climate. Glob. Chang. Biol. 6, 801–817.

Beaulieu, C., Henson, S.A., Sarmiento, J.L., Dunne, J.P., Doney, S.C., Rykaczewski, R.R., Bopp, L., 2013. Factors challenging our ability to detect long-term trends in ocean chlorophyll. Biogeosciences 10 (4), 2711–2724. http://dx.doi.org/10.5194/bg-10-2711-2013.

Behrenfeld, M.J., O'Malley, R.T., Siegel, D.A., McClain, C.R., Sarmiento, J.L., Feldman, G.C., Milligan, A.J., Falkowski, P.G., Letelier, R.M., Boss, E.S., 2006. Climate-driven trends in contemporary ocean productivity. Nature 444. http://dx.doi.org/10.1038/nature05317.

Boyce, D.G., Lewis, M.R., Worm, B., 2010. Global phytoplankton decline over the past century. Nature 466 (7306), 591–596.

Boyce, D.G., Lewis, M., Worm, B., 2012. Integrating global chlorophyll data from 1890 to 2010. Limnol. Oceanogr. Methods 10, 840–852.

Boyce, D.G., Dowd, M., Lewis, M., Worm, B., 2014. Estimating global chlorophyll changes over the past century. Prog. Oceanogr. 122, 163–173.

Brewin, R.J.W., Sathyendranath, S., Hirata, T., Lavender, S.J., Barciela, R.M., Hardman-Mountford, N.J., 2010. A three-component model of phytoplankton size class for the Atlantic Ocean. Ecol. Model. 221 (11), 1472–1483.

Brewin, R.J.W., Devred, E., Sathyendranath, S., Hardman-Mountford, N.J., Lavender, S.J., 2011. Model of phytoplankton absorption based on three size classes. Appl. Opt. 50, 4535–4549. http://dx.doi.org/10.1364/AO.50.004535.

Brewin, R.J.W., Hirata, T., Hardman-Mountford, N.J., Lavender, S., Sathyendranath, S., Barlow, R., 2012. The influence of the Indian Ocean Dipole on interannual variations in phytoplankton size structure as revealed by Earth Observation. Deep-Sea Res. II 77–80, 117–127.

Brewin, R.J.W., Sathyendranath, S., Lange, P.K., Tilstone, G., 2014a. Comparison of two methods to derive the size-structure of natural populations of phytoplankton. Deep-Sea Res. I 85, 72–79. http://dx.doi.org/10.1016/j.dsr.2013.11.007.

Brewin, R.J.W., Sathyendranath, S., Tilstone, G., Lange, P.K., Platt, T., 2014b. A multicomponent model of phytoplankton size structure. J. Geophys. Res. Oceans 119. http://dx.doi.org/10.1002/2014JC009859.

Brewin, R.J.W., Mélin, F., Sathyendranath, S., Steinmetz, F., Chuprin, A., Grant, M., 2014c. On the temporal consistency of chlorophyll products derived from three ocean-colour sensors. ISPRS J. Photogramm. Remote Sens. 97, 171–184. http://dx.doi.org/10.1016/j.isprsjprs.2014.08.013.

Brotas, V., Brewin, R.J.W., Sá, C., Brito, A., Silva, A., Mendes, C.R., Diniz, T., Kaufmann, M., Tarran, G., Groom, S.B., Platt, T., Sathyendranath, S., 2013. Deriving phytoplankton size classes from satellite data: validation along a trophic gradient in the eastern Atlantic Ocean. Remote Sens. Environ. 134, 66–77. http://dx.doi.org/10.1016/j.rse.2013.02.013.

Budge, S.M., Devred, E., Forget, M.-H., Stuart, V., Trzcinski, M.K., Sathyendranath, S., Platt, T., 2014. Estimating concentrations of essential omega-3 fatty acids in the ocean: supply and demand. ICES J. Mar. Sci. http://dx.doi.org/10.1093/icesjms/fsu003.

Chassot, E., Bonhommeau, S., Dulvy, N.K., Mélin, F., Watson, R., Gascuel, D., Le Pape, O., 2010. Global marine primary production constrains fisheries catches. Ecol. Lett. 13, 495–505.

Chisholm, S.W., 1992. Phytoplankton size. In: Falkowski, P.G., Woodhead, A.D. (Eds.), Primary Productivity and Biogeochemical Cycles in the Sea. Springer, New York, pp. 213–237.

Ciotti, A.M., Lewis, M.R., Cullen, J.J., 2002. Assessment of the relationships between dominant cell size in natural phytoplankton communities and the spectral shape of the absorption coefficient. Limnol. Oceanogr. 47, 404–417.

Cury, P.M., Shin, Y.-J., Planque, B., Durant, J.M., Fromentin, J.-M., Kramer-Schadt, S., Stenseth, N.C., Travers, M., Grimm, V., 2008. Ecosystem oceanography for global change in fisheries. Trends Ecol. Evol. 23, 338–346.

Devred, E., Sathyendranath, S., Stuart, V., Platt, T., 2011. A three component classification of phytoplankton absorption spectra: applications to ocean colour data. Remote Sens. Environ. 115 (9), 2255–2266.

Dierssen, H.M., 2010. Perspectives on empirical approaches for ocean color remote sensing of chlorophyll in a changing climate. Proc. Natl. Acad. Sci. U. S. A. 107 (40), 17073–17078. http://dx.doi.org/10.1073/pnas.0913800107.

Dugdale, R.C., Wilkerson, F.P., Chai, F., Feely, R., 2007. Size-fractionated nitrogen uptake in the equatorial Pacific and conformation of the low Si-high-nitrate low-chlorophyll condition. Glob. Biogeochem. Cycles 21 (2), GB2005. http://dx.doi.org/10.1029/2006BG002722.

Falkowski, P.G., 1997. Evolution of the nitrogen cycle and its influence on the biological sequestration of CO_2 in the ocean. Nature 387, 272–275.

Field, C.B., Behrenfeld, M.J., Randerson, J.T., Falkowski, P., 1998. Primary production of the biosphere: integrating terrestrial and oceanic components. Science 281 (5374), 237–240.

Gibb, S.W., Barlow, R.G., Cummings, D.G., Rees, N.W., Trees, C.C., Holligan, P., Suggett, D., 2000. Surface phytoplankton pigment distributions in the Atlantic Ocean: an assessment of basin scale variability between 50 degrees N and 50 degrees S. Prog. Oceanogr. 45 (3–4), 339–368.

Gordon, H.R., McCluney, W.R., 1975. Estimation of depth of sunlight penetration in sea for remote-sensing. Appl. Opt. 14 (2), 413–416.

Gregg, W.W., Casey, N.W., 2010. Improving the consistency of ocean color data: a step toward climate data records. Geophys. Res. Lett. 37, L04605. http://dx.doi.org/10.1029/2009GL041893.

Gregg, W.W., Conkright, M.E., 2002. Decadal changes in global ocean chlorophyll. Geophys. Res. Lett. 29 (15).

Gregg, W.W., Rousseaux, C.S., 2014. Decadal trends in global pelagic ocean chlorophyll: a new assessment integrating multiple satellites, *in-situ* data, and models. J. Geophys. Res. Oceans 119, 5921–5933. http://dx.doi.org/10.1002/2014JC010158.

Guidi, L., Stemmann, L., Jackson, G.A., Ibanez, F., Claustre, H., Legendre, L., Picheral, M., Gorskya, G., 2009. Effects of phytoplankton community on production, size and export of large aggregates: a world-ocean analysis. Limnol. Oceanogr. 54 (6), 1951–1963.

Hardman-Mountford, N.J., Hirata, T., Richardson, K.A., Aiken, J., 2008. An objective methodology for the classification of ecological pattern into biomes and provinces for the pelagic ocean. Remote Sens. Environ. 112, 3341–3352.

Henson, S.A., Sarmiento, J.L., Dunne, J.P., Bopp, L., Lima, I., Doney, S.C., John, J., Beaulieu, C., 2010. Detection of anthropogenic climate change in satellite records of ocean chlorophyll and productivity. Biogeosciences 7, 621–640. http://dx.doi.org/10.5194/bg-7-621-2010.

Hirata, T., Hardman-Mountford, N.J., Brewin, R.J.W., Aiken, J., Barlow, R., Suzuki, K., Isada, T., Howell, E., Hashioka, T., Noguchi-Aita, M., Yamanaka, Y., 2011. Synoptic relationships between surface chlorophyll-a and diagnostic pigments specific to phytoplankton functional types. Biogeosciences 8, 311–327.

Hooker, S.B., McClain, C.R., 2000. The calibration and validation of SeaWiFS data. Prog. Oceanogr. 45 (3–4), 427–465.

IOCCG, 2014. Phytoplankton functional types from space. In: Sathyendranath, S. (Ed.), Reports of the International Ocean-Colour Coordinating Group, No. 15, IOCCG, Dartmouth, Canada.

Jackson, T., Bouman, H.A., Sathyendranath, S., Devred, E., 2011. Regional-scale change in diatom distribution in the Humboldt upwelling system as revealed by remote sensing: implications for fisheries. ICES J. Mar. Sci. 68, 729–736.

Jeffrey, S.W., Wright, S.W., Zapata, M., 2011. Microalgal classes and their signature pigments. In: Roy, S., Llewellyn, C.A., Egeland, E.S., Johnsen, G. (Eds.), Phytoplankton Pigments. Cambridge University Press, pp. 3–77.

Kostadinov, T.S., Siegel, D.A., Maritorena, S., 2010. Global variability of phytoplankton functional types from space: assessment via the particle size distribution. Biogeosciences 7, 3239–3257.

Kröger, N., Deautzmann, R., Bergsdorf, C., Sumper, M., 2000. Species-specific polyamines from diatoms control silica morphology. Proceedings of the National Academy of the United States of America 97 (26), 14133–14138. http://dx.doi.org/10.1073/pnas.260496497.

Laws, E.A., Falkowski, P.G., Smith Jr., W.O., Ducklow, H., McCarth, J.J., 2000. Temperature effects on export production in the open ocean. Glob. Biogeochem. Cycles 14, 1231–1246.

Le Quéré, C., Harrison, S.P., Prentice, C.I., Buitenhuis, E.T., Aumont, O., Bopp, L., Claustre, H., Cotrim Da Cunha, L., Geider, R., Giraud, X., Klaas, C., Kohfeld, K.E., Legendre, L., Manizza, M., Platt, T., Rivkin, R., Sathyendranath, S., Uitz, J., Watson, A.J., Wolf-Gladrow, D., 2005. Ecosystem dynamics based on plankton functional types for global ocean biogeochemistry models. Glob. Chang. Biol. 11 (11), 2016–2040.

Liss, P., Malin, G., Turner, S.M., Holligan, P.H., 1994. Dimethyl sulphide and *Phaeocystis*: a review. J. Mar. Syst. 5, 41–53.

Llewellyn, C.A., White, D.A., Martinez-Vincente, V., Tarran, G.A., Smyth, T.J., 2012. Distribution of mycosporine-like amino acids along a surface water meridional transect of the Atlantic. Microbiol. Aquat. Syst. 64, 320–333.

Longhurst, A., 2007. Ecological Geography of the Sea. Academic Press.

Longhurst, A., Sathyendranath, S., Platt, T., Caverhill, C., 1995. An estimate of global primary production in the ocean from satellite radiometer data. J. Plankton Res. 17 (6), 1245–1271.

Mackas, D.L., 2011. Does blending of chlorophyll data bias temporal trend? Nature 472 (7342), E4–E5.

Maloney, C.L., Field, J.G., 1991. The size-based dynamics of plankton food webs. I. A simulation model of carbon and nitrogen flows. J. Plankton Res. 13 (5), 1003–1038.

Marañón, E., 2009. Phytoplankton size structure. In: Steele, J.H., Turekian, K., Thorpe, S.A. (Eds.), Encyclopedia of Ocean Sciences. Academic Press, Oxford.

Marañón, E., Cermeño, P., Latasa, M., Tadonléké, R.D., 2012. Temperature, resources, and phytoplankton size structure in the ocean. Limnol. Oceanogr. 57, 1266–1278.

Martinez, E., Antoine, D., D'Ortenzio, F., Gentili, B., 2009. Climate-driven basin scale decadal oscillations of oceanic phytoplankton. Science 326, 1253–1256. http://dx.doi.org/10.1126/science.1177012.

McQuatters-Gollop, A., Reid, P.C., Edwards, M., Burkill, P.H., Castellani, C., Batten, S., Gieskes, W., Beare, D., Bidigare, R.R., Head, E., Johnson, R., Kahru, M., Koslow, J.A., Pena, A., 2011. Is there a decline in marine phytoplankton? Nature 472 (7342), E6–E7.

Morel, A., Huot, Y., Gentili, B., Werdell, P.J., Hooker, S.B., Franz, B.A., 2007. Examining the consistency of products derived from various ocean color sensors in open ocean (case 1) waters in the perspective of a multi-sensor approach. Remote Sens. Environ. 111, 69–88.

Morse, J.W., Arvidson, R.S., Lüttge, A., 2007. Calcium carbonate formation and dissolution. Chem. Rev. 107 (2), 342–382.

O'Reilly, J.E., Maritorena, S., Mitchell, B.G., Siegel, D.A., Carder, K.L., Garver, S.A., Kahru, M., McClain, C., 1998. Ocean chlorophyll algorithms for SeaWiFS. J. Geophys. Res. 103 (C11), 24,937–24,953.

Platt, T., Sathyendranath, S., 2008. Ecological indicators for the pelagic zone of the ocean from remote sensing. Remote Sens. Environ. 112, 3426–3436.

Poulton, A.J., Holligan, P.M., Hickman, A., Kim, Y.-N., Adey, T.R., Stinchcombe, M.C., Holeton, C., Root, S., Woodward, E.M.S., 2006. Phytoplankton carbon fixation, chlorophyll-biomass and diagnostic pigments in the Atlantic Ocean. Deep-Sea Res. II Top. Stud. Oceanogr. 53 (14–16), 1593–1610.

Racault, M.-F., Le Quéré, C., Buitenhuis, E., Sathyendranath, S., Platt, T., 2012. Phytoplankton phenology in the global ocean. Ecol. Indic. 14 (1), 152–163. http://dx.doi.org/10.1016/j.ecolind.2011.07.010.

Racault, M.-F., Sathyendranath, S., Platt, T., 2014a. Impact of missing data on the estimation of ecological indicators from satellite ocean-colour time-series. Remote Sens. Environ. 152, 15–28. http://dx.doi.org/10.1016/j.rse.2014.05.016.

Racault, M.-F., Platt, T., Sathyendranath, S., Agirbas, E., Martinez-Vicente, V., Brewin, R.J.W., 2014b. Plankton indicators and ocean observing systems: support to the marine ecosystem state assessment. J. Plankton Res. 36, 621–629. http://dx.doi.org/10.1093/plankt/fbu016.

Raitsos, D.E., Reid, P.C., Lavender, S.J., Edwards, M., Richardson, A.J., 2005. Extending the SeaWiFS chlorophyll data set back 50 years in the northeast Atlantic. Geophys. Res. Lett. 32, 1–4.

Raitsos, D.E., Pradhan, Y., Lavender, S.J., Hoteit, I., McQuatters-Gollop, A., Reid, P.C., Richardson, A.J., 2014. From silk to satellite: half a century of ocean colour anomalies in the Northeast Atlantic. Glob. Chang. Biol. 20, 2117–2123. http://dx.doi.org/10.1111/gcb.12457.

Robinson, C., Poulton, A.J., Holligan, P.M., Baker, A.R., Forster, G., Gist, N., Jickells, T.D., Malin, G., Upstill-Goddardd, R., Williams, R.G., Woodward, E.M.S., Zubkov, M.V., 2006. The Atlantic Meridional Transect (AMT) Programme: a contextual view 1995–2005. Deep-Sea Res. II 53, 1485–1515.

Siegel, D.A., Behrenfeld, M.J., Maritorena, S., McClain, C.R., Antoine, D., Bailey, S.W., Bontempi, P.S., Boss, E.S., Dierssen, H.M., Doney, S.C., Eplee Jr., R.E., Evans, R.H., Feldman, G.C., Fields, E., Franz, B.A., Kuring, N.A., Mengelt, C., Nelson, N.B., Patt, F.S., Robinson, W.D., Sarmiento, J.L., Swan, C.M., Werdell, P.J., Westberry, T.K., Wilding, J.G., Yoder, J.A., 2013. Regional to global assessments of phytoplankton dynamics from the SeaWiFS mission. Remote Sens. Environ. 135, 77–91. http://dx.doi.org/10.1016/j.rse.2013.03.025.

Sokal, R.R., Rohlf, F.J., 1969. Biometry: the principles and practice of statistics in biological research. W.H. Freeman, San Francisco 776 p. Department of Ecology and Evolution, State University of New York, Stony Brook, NYJ.

Takahashi, T., Sutherland, S.C., Sweeney, C., Poisson, A., Metzl, N., Tilbrook, B., Bates, N., Wanninkhof, R., Feely, R.A., Sabine, C., Olafsson, J., Nojiri, Y., 2002. Global sea-air CO_2 flux based on climatological surface ocean pCO_2 and seasonal biological and temperature effects. Deep-Sea Res. II 49, 1601–1622.

Tilstone, G.H., Airs, R.L., Martinez-Vicente, V., Widdicombe, C., Llewellyn, C., 2010. High concentrations of mycosporine-like amino acids and colored dissolved organic matter in the sea surface microlayer off the Iberian Peninsula. Limnol. Oceanogr. 55 (5), 1835–1850.

Tyrrell, T., 1999. The relative influences of nitrogen and phosphorus on oceanic primary production. Nature 400, 525–531.

Uitz, J., Claustre, H., Morel, A., Hooker, S.B., 2006. Vertical distribution of phytoplankton communities in open ocean: an assessment based on surface chlorophyll. J. Geophys. Res. Oceans 111 (C8).

Uitz, J., Huot, Y., Bruyant, F., Babin, M., Claustre, H., 2008. Relating phytoplankton photophysiological properties to community structure on large scales. Limnol. Oceanogr. 53 (2), 614–630.

Uitz, J., Claustre, H., Gentili, B., Stramski, D., 2010. Phytoplankton class-specific primary production in the world's oceans: seasonal and interannual variability from satellite observations. Glob. Biogeochem. Cycles 24, GB3016.

Vantrepotte, V., Mélin, F., 2009. Temporal variability of 10-year global SeaWiFS time-series of phytoplankton chlorophyll a concentration. ICES J. Mar. Sci. 66, 1547–1556.

Vantrepotte, V., Mélin, F., 2011. Inter-annual variations in the SeaWiFS global chlorophyll a concentration (1997–2007). Deep-Sea Res. I 58, 429–441.

Vidussi, F., Claustre, H., Manca, B.B., Luchetta, A., Marty, J.C., 2001. Phytoplankton pigment distribution in relation to upper thermocline circulation in the eastern Mediterranean Sea during winter. J. Geophys. Res. Oceans 106 (C9), 19939–19956.

Wolter, K., Timlin, M.S., 1998. Measuring the strength of ENSO events: how does 1997/98 rank? Weather 53 (9), 315–324. http://dx.doi.org/10.1002/j.1477-8696.1998.tb06408.x.